https://doi.org/10.5194/acp-2019-1182
Preprint. Discussion started: 28 January 2020

Atmospheric Chemistry and Physics Discussions

Modelling mixed-phase clouds with large-eddy model UCLALES-SALSA

Jaakko Ahola[1], Hannele Korhonen[1], Juha Tonttila[2], Sami Romakkaniemi[2], Harri Kokkola[2], and Tomi Raatikainen[1]

[1]Finnish Meteorological Institute, Helsinki, Finland
[2]Finnish Meteorological Institute, Kuopio, Finland

Correspondence: Jaakko Ahola (jaakko.ahola@fmi.fi)

Abstract. The large-eddy model UCLALES-SALSA, with exceptionally detailed aerosol description for both aerosol number and chemical composition, has been extended for ice and mixed-phase clouds. Comparison to a previous mixed-phase cloud model intercomparison study confirmed the accuracy of newly implemented ice microphysics. Further simulation with a heterogeneous ice nucleation scheme, where also ice nucleating particles (INP) are a prognostic variable, captured the typical layered structure of Arctic mid-altitude mixed-phase cloud: a liquid layer near cloud top and ice within and below the liquid layer. In addition, the simulation showed realistic freezing rate of droplets within the vertical cloud structure. The represented detailed sectional ice microphysics with prognostic aerosols is crucially important in reproducing mixed-phase clouds.

1 Introduction

Clouds are known to have a prominent influence on the hydrological cycle and the atmospheric radiation balance. While significant advances have been made in characterisation of liquid-phase clouds, the microphysical processes, especially heterogeneous ice nucleation, dynamics and radiative effects of mixed-phase and ice clouds remain more poorly constrained. This is mainly because of challenges in obtaining representative observations and a lack of a detailed enough representation of microphysics in climate and numerical weather prediction models. Specific challenges are known to be associated with aerosol-cloud interactions (Cox, 1971; Knight and Heymsfield, 1983; CUR; Solomon et al., 2007; Stevens and Feingold, 2009; Morrison et al., 2011a; Morrison, 2012; Li et al., 2013).

What we know about mixed-phase clouds is that by definition supercooled liquid droplets coexist with ice crystals. Such clouds are frequent at temperatures between $-10°C$ and $-25°C$ (Filioglou et al., 2019), but can be present from $-35°C$ to $0°C$ and require specific microphysical and dynamical conditions (Andronache, 2017). Ice crystals can form either by homogeneous or heterogeneous freezing (term *nucleation* used also). In temperatures lower than $-38°C$, liquid droplets can freeze homogeneously without the need of ice nucleating particles (INP). In heterogeneous ice nucleation, freezing initiates from the surface of seed particle and can occur at higher temperatures than homogeneous ice nucleation. Droplet freezing processes are not yet fully understood and quantified despite of decades of research (Phillips et al., 2008; Atkinson et al., 2013; DeMott et al., 2011). Kiselev et al. (2017) stated that ice formation on aerosol particles (heterogeneous ice nucleation) is a

https://doi.org/10.5194/acp-2019-1182
Preprint. Discussion started: 28 January 2020

Atmospheric Chemistry and Physics Discussions

process of crucial importance to Earth's climate, but it is not understood at the molecular level. However, in Morrison et al. (2011a) it is noted that although many details of droplet freezing are poorly understood, enough knowledge exists to draw first-order (ice water path) conclusions. Furthermore, droplet freezing models and even the representation of cloud structure often require a resolution that is too detailed for large scale models. For instance, the structure of Arctic and mid-altitude clouds is complex with a layered structure with liquid near cloud top and ice within and below the liquid layer (Curry et al., 1997; Hobbs and Rangno, 1998; Pinto, 1998; Rangno and Hobbs, 2001; Zuidema et al., 2005; Shupe et al., 2006; Verlinde et al., 2007; de Boer et al., 2009; McFarquhar et al., 2011; Morrison et al., 2011a). The lack of a proper calculation of ice processes in climate models is seen in the comparisons to observations of mid- and high-latitude mixed-phase clouds. These models tend to underestimate the lifetime of such clouds (Andronache, 2017). Better quantification of droplet freezing processes is expected to narrow the gap between observations and model results.

The importance of including detailed aerosol description is vital in cloud resolving models. Scarcity of INP is an important factor in mixed-phase clouds lifetime and structure, since roughly one in a million particles acts as an ice nucleus and even these particles might have highly different ice-forming activity at different temperatures (Lebo et al., 2008; Morrison et al., 2011a). Therefore, the loss of INP along with precipitating ice crystals limits cloud glaciation and dissipation (Rauber and Tokay, 1991; Harrington et al., 1999; Avramov and Harrington, 2010). Describing this process is not possible without detailed description of aerosols, as is demonstrated in a 1-D cloud model study by Morrison et al. (2005). The significance of aerosols is shown in Filioglou et al. (2019) where high aerosol load was linked with a more likely presence of liquid phase in Arctic clouds. Also, the Norgren et al. (2018) study shows how there is less ice in polluted clouds. Andronache (2017) and Morrison et al. (2011a) are comprehensive review resources to give more further details about mixed-phase clouds.

There is a growing number of studies focusing on examining the properties of mixed-phase or ice clouds by combining observations and models, including large eddy simulation (LES) modelling and other cloud-resolving models (CRM) (Jiang et al., 2000; Klein et al., 2009; Morrison et al., 2011b; Ovchinnikov et al., 2014; Andronache, 2017). Large-eddy simulations are particularly attractive for modelling boundary layer clouds since they offer a good compromise between computational cost and accuracy in terms of model resolution (Tonttila et al., 2017; Andronache, 2017). LES models solve the largest eddies in turbulent flows explicitly and use parameterisations for the smallest length scales. In atmospheric applications they are usually coupled with cloud microphysical packages. Recent developments in computational performance of supercomputers have made explicit and detailed description of aerosol-cloud-ice microphysical interactions possible also in LES modelling, allowing the investigation of non-linear cloud phenomena, such as secondary ice production and heterogeneous ice nucleation.

There are several LES models that solve cloud related interactions (Fridlind et al., 2012; Khain et al., 2004; Savre and Ekman, 2015; Fu and Xue, 2017). In comparison to those models, we present a LES model UCLALES-SALSA that brings additional value with a more detailed aerosol description. UCLALES-SALSA explicitly resolves interactions between aerosols, ice crystals and cloud droplets with sectional microphysics for all hydrometeors while keeping track of the aerosol dry size distribution. Sectional description, especially for aerosols, is a clear asset of UCLALES-SALSA and we have now extended this description also for ice crystals. This sectional aerosol description allowed the implementation of a detailed heterogeneous

https://doi.org/10.5194/acp-2019-1182
Preprint. Discussion started: 28 January 2020

Atmospheric Chemistry and Physics Discussions

freezing processes. First, the model results are compared with previously published modelling results. Finally, we demonstrate the benefits of this approach to handle heterogeneous freezing over more simplified aerosol-ice-cloud treatments.

2 Model description

The UCLALES-SALSA (Tonttila et al., 2017) model consists of two components: first, the widely used large eddy simulator UCLALES that handles the atmospheric dynamics including turbulence (Stevens et al., 1999, 2005), and second the aerosol bin microphysics model SALSA (Sectional Aerosol module for Large-Scale Applications) (Kokkola et al., 2008; Tonttila et al., 2017; Kokkola et al., 2018). The previous version of UCLALES-SALSA incorporated interactions between aerosols, clouds and drizzle (Tonttila et al., 2017). Now we have extended the model with a description for ice crystals. In this study, we focus on how ice crystals and ice nucleating particles (INP) interact with clouds while tracking sectional aerosol size distribution.

Figure 1 illustrates the treatment of different hydrometeor classes and their size distributions in UCLALES-SALSA. All four classes (aerosol, cloud and rain droplets and ice crystals) are tracked with a bin scheme. Bin scheme offers the benefit of greater accuracy in simulating interactions between different sized hydrometeors. Better accuracy is gained by dividing the size distribution into bins. This also enables better flexibility as the shape of the distribution is allowed to evolve. Bulk schemes provide a simpler method and track one or several moments of the size distribution, where the shape of distribution is prescribed. The disadvantage of bin scheme is higher computational cost compared to bulk scheme.

Three of the hydrometeor classes, i.e. aerosol, cloud droplets and ice, are further divided into parallel bins labelled a and b as shown in Fig. 1. This division into a and b bins is done to enable the tracking of externally mixed distributions and to see how different particles affect clouds. For aerosol particles, subrange 1a is an additional feature to describe nucleation mode. Otherwise, Aitken and accumulation mode size ranges are sufficient to characterise cloud phenomena.

The aerosol, cloud and ice crystal size distributions are discretised into the bins according to the dry aerosol diameter, whereas the rain droplet size distribution is defined by the wet diameter of the droplet. Identical 2a and 2b size bins are used for aerosol, cloud droplets and ice. Such parallel bins are useful for tracking aerosol development through cloud activation and freezing. Prognostic variables for each bin include aerosol number and masses of all compounds (water, sulphate, dust, organic carbon, sea salt, nitrate, and ammonium).

In UCLALES-SALSA, recently implemented processes involving ice crystals are droplet freezing, deposition of water vapour, sublimation, melting, coagulation between different sized hydrometeors, sedimentation, and interactions with radiation (see also Fig. 1). Most of these processes are included in the same way as in the previously published version of UCLALES-SALSA (Tonttila et al., 2017). For instance, interaction with radiation is implemented with the same four-stream radiative transfer solver (Fu and Liou, 1993) as before but extended to include ice crystals. Condensation of water vapour to ice crystals is based on the analytical predictor of condensation (APC) scheme by Jacobson (2005) and implemented following Tonttila et al. (2017) (Eqs. 7 and 8). For solids, the condensation does not require Kelvin or Roult terms. Furthermore, UCLALES-SALSA was upgraded with minor bug fixes and improvements. For example, hygroscopicity is now calculated with κ-Köhler (Petters et al., 2006; Petters and Kreidenweis, 2007) instead of previously used ZSR method (Stokes and Robinson, 1966).

https://doi.org/10.5194/acp-2019-1182
Preprint. Discussion started: 28 January 2020


Atmospheric Chemistry and Physics Discussions

Regarding the scope of this study, we describe droplet freezing in higher detail. There are five mechanisms for droplet freezing and they are all currently implemented in UCLALES-SALSA.

- Immersion freezing is possible for aqueous droplets that have an insoluble core, which in UCLALES-SALSA is either dust (DU) or black carbon (BC). The rate of heterogeneous germ formation in a supercooled droplet of water or solution is calculated mostly following Khvorostyanov and Curry (2000) and additional parameters are from Jeffery and Austin (1997), Khvorostyanov and K. Sassen (1998), Khvorostyanov and Curry (2004) and Li et al. (2013).
- Homogeneous freezing is possible for any aqueous droplet with or without insoluble particles. This is applied to the model according to Khvorostyanov and K. Sassen (1998).
- Deposition freezing is possible for dry insoluble aerosol at sub-saturated conditions ($RH < 100\%$). This is implemented following Khvorostyanov and Curry (2000) and additional parameters from Hoose et al. (2010).
- Contact freezing is implemented in UCLALES-SALSA following Hoose et al. (2010) so that first the coagulation code is used to calculate collision rates between dry particles and liquid droplets and then immersion freezing code gives the freezing probability.
- Condensation freezing is implemented as a part of immersion freezing, because these droplets can freeze during the modelled condensational growth.

In our simulations (Sect. 3.3), only immersion freezing is active. This is done to keep the intercomparison simple enough and also due to high temperatures when immersion freezing is the dominant freezing mechanism. A more detailed description of the treatment of immersion freezing is given in Appendix A.

3 Results

3.1 Model evaluation

The model performance is evaluated by simulating a well-documented mixed-phase cloud case from the Indirect and Semi-Direct Aerosol Campaign (ISDAC) Arctic study (McFarquhar et al., 2011). This observation case has been used before for comparisons to LES-models (e.g., Savre and Ekman, 2015; Fu and Xue, 2017). Ovchinnikov et al. (2014) presented an intercomparison of 11 LES models for this same case, where initial profiles were based on aircraft observations in the mixed layer (Flight F31) and idealisation of a sounding on 26th April 2008 at Barrow, AK. Nine of those models had bulk 2-moment microphysics and two of them bin microphysics.

We implemented in UCLALES-SALSA model runs the same semi-idealised simulation setup given in Ovchinnikov et al. (2014) that attempted to minimise intermodel differences by applying identical descriptions for the following processes: surface properties and fluxes (fluxes set to zero), large-scale forcings, radiation, cloud droplet freezing and ice growth processes and sedimentation, and the nudging of horizontal winds, potential temperature and water content above the altitude of 1200 m.

https://doi.org/10.5194/acp-2019-1182
Preprint. Discussion started: 28 January 2020

Atmospheric Chemistry and Physics Discussions

In the simulations ice processes were excluded during the first two hours, i.e. the spinup period, to allow the mixed-layer turbulence and the warm stratus cloud to develop. After the spinup, cloud droplets are allowed to freeze until a specified target ice concentration is reached (Morrison et al., 2011b). Ice shape is described with a mass-diameter parameterisation so that ice can be considered as spherical particles with low effective density ($\rho = 84.5\ \mathrm{kg\ m^{-3}}$). Ice fall speed is related to the maximum dimension while capacitance, which is used in the condensation equation, is modified from that of a sphere to $C = D/\pi$. Radiation and sedimentation were parameterised similar to Ovchinnikov et al. (2014). For the sake of simplicity, coagulation was switched off as in Ovchinnikov et al. (2014). Warm rain formation was switched off allowing more straightforward model intercomparison. Also, the warm rain mass mixing ratios would have been small due to relatively small cloud droplet size in the simulated case. Aerosol size distribution is given as a sum of lognormal accumulation and coarse modes with concentrations of 159e6 and 6.5e6 $\mathrm{kg^{-1}}$, mode mean diameters of 0.2 and 0.7 $\mu\mathrm{m}$ and geometric standard deviations of 1.5 and 2.45, respectively. Aerosol is composed of ammonium bisulphate. During the simulations this aerosol size distribution provides on average 129e6 $\mathrm{kg^{-1}}$ cloud droplets.

We ran UCLALES-SALSA for the three different simulation setups investigated in the Ovchinnikov et al. (2014) study: no ice (ICE0), average ice (ICE1) and high ice (ICE4) number concentration. The ice number concentration is the only variable that was changed between the evaluation simulations (either 0, 1 or 4 $\mathrm{L^{-1}}$). Liquid and ice water paths (marked LWP and IWP from now on), i.e. column integrated mass values averaged over the horizontal domain, in these three cases show how water is distributed between ice and liquid phases depending on the ice crystal concentration.

Figure 2 compares the three UCLALES-SALSA simulations to the results presented in the Ovchinnikov et al. (2014) intercomparison paper. In the figure, LES model results from Ovchinnikov et al. (2014) are separated between bulk and bin microphysics to highlight the differences between microphysics schemes. First, Fig. 2a shows LWP for the baseline simulation without any ice (ICE0). It is evident that our model agrees well with the other 11 models. The simulated LWP of UCLALES-SALSA is in the middle of the model spread. Differences are most likely explained by different dynamical cores, which is stated also in Ovchinnikov et al. (2014). A more thorough testing of warm phase cloud microphysics in UCLALES-SALSA was done in the Tonttila et al. (2017), and for the remainder of this work we will concentrate on examining the properties of the ice microphysics implementation.

Second, Figs. 2b and 2c present the LWP and IWP time series, when the target ice number concentration is 1 $\mathrm{L^{-1}}$, marked with ICE1. Again, LWP in UCLALES-SALSA matches well with the other models being in the lower end of the intermodel spread. As expected, the LWP growth rate is lower than in ICE0 simulation, as some of the water vapour condenses onto ice crystals. Furthermore, IWP matches well especially with other bin models in the Ovchinnikov et al. (2014) study.

Third, Fig. 2d depicts LWP time series with ice number concentration of 4 $\mathrm{L^{-1}}$, which can be regarded as high ice concentration and is marked with ICE4. Now after spinup, LWP has a decreasing trend since the ice number concentration is so high that it consumes much of the water vapour. Subsequently, IWP in Fig. 2e increases rapidly after the spinup and in UCLALES-SALSA reaches its peak value of 15.7 $\mathrm{g\ m^{-2}}$ just before 4 hours of simulation. It then decreases to a value of 9.4 $\mathrm{g\ m^{-2}}$ at the end of the simulation. The reduction of IWP is caused by ice crystal precipitation at the surface and evaporation below the cloud.

https://doi.org/10.5194/acp-2019-1182
Preprint. Discussion started: 28 January 2020

Atmospheric Chemistry and Physics Discussions

Compared to the model results in Ovchinnikov et al. (2014), IWP in UCLALES-SALSA declines faster after the peak IWP has been reached in ICE4. One reason for this is that dry particle size is tracked in UCLALES-SALSA and this seem to have an important effect on ice crystal sedimentation. The other reason is related to the model dependent technical details such as the advection flux limiter method. In Ovchinnikov et al. (2014) it was also stated that when the ice number concentration gets higher the differences between models are more caused by discrepancies in microphysics than cloud dynamics. This underlines the sensitivity and significance of microphysics.

To conclude, the spread between models, especially between bin and bulk microphysics models, gets wider as the prescribed ice number concentration gets larger and closer to the limit when the cloud glaciates completely. In UCLALES-SALSA this limit of full glaciation is lower than in other models in Ovchinnikov et al. (2014). This limit is further examined in Sect. 3.2.

3.2 Sensitivity on ice concentration

Motivated by simulated differences with the 4 L^{-1} ice concentration, we wanted to further investigate how sensitive cloud glaciation is to changes in ice number concentration. In addition to ICE1 and ICE4 simulations, we performed simulations in which the target ice number concentration was 2, 3, 5 or 6 L^{-1} (marked with ICE2, ICE3, ICE5 and ICE6 respectively). Figure 3 depicts the LWP and IWP evolution in all six UCLALES-SALSA simulations. The simulation time was extended to 24 hours in those cases where cloud still exists after 8 hours (marked with vertical line in Fig. 3). The simulation time was not extended any further, because we do not see any major changes or trends in the last simulation hours.

Figure 3 shows that when the ice number concentration is set to a higher value, LWP decreases faster and cloud glaciates sooner. In simulations ICE4, ICE5 and ICE6, the cloud dissipates totally after glaciation. The cloud glaciation happens because water vapour condenses on the ice crystals at the expense of the cloud droplets. In simulations ICE1, ICE2 and ICE3, IWP stabilises to values of approximately 6.5, 10 and 12 $\mathrm{g\ m}^{-2}$ respectively towards the end of simulation.

From Fig. 3 we can also see that LWP still increases during the first 8 hours with ICE2 but not anymore with ICE3. With ICE1, the water paths of the cloud are very stable after 8 hours of simulation. LWP decreases about 2 $\mathrm{g\ m}^{-2}$ reaching a value of 44 $\mathrm{g\ m}^{-2}$ at the end of simulation. IWP is around 7 $\mathrm{g\ m}^{-2}$ at the end of simulation. LWP values for ICE2 and ICE3 simulations are around 22 and 18 $\mathrm{g\ m}^{-2}$, and IWP values are 10 and 12 $\mathrm{g\ m}^{-2}$ at the end of simulation, respectively. These are close to ICE4 simulations presented in Ovchinnikov et al. (2014), and this illustrates the fine balance between co-existing liquid and ice phases.

These results show how sensitive the mixed-phase cloud is to ice number concentration either by showing how fast the cloud glaciates or when balance is reached. However, these are highly simplified due to the lack or real aerosol dependent freezing and related feedback processes. These results also show the need for more detailed feedbacks since constant ice number concentration is not a realistic assumption for real clouds.

3.3 Prognostic ice simulation

One of the unique features of our model is its ability to keep track of the chemical composition along with sectional aerosol size distribution also in cloud phase. This allows us to model freezing processes related to an ice nucleating compound like

https://doi.org/10.5194/acp-2019-1182
Preprint. Discussion started: 28 January 2020

Atmospheric Chemistry and Physics Discussions

dust. Furthermore, parallel bins allow for analysing the relative contribution of e.g. dust particles (INP) on ice formation. We call this prognostic ice because here freezing probability is related to dust aerosol which mass and number concentrations are prognostic variables. We allow interactions between all hydrometeors and ice formation is modelled using the implemented ice nucleation theories, which relate ambient conditions and droplet properties to their freezing rates.

To see the difference between fixed and prognostic droplet freezing, we made a prognostic ice simulation that was targeted to have similar IWP during the first 8 hours as in the simulation with ice number concentration of 4 L^{-1} (ICE4) (see Sections 3.1 and 3.2). This ICE4 simulation was selected for comparison because it is close to the tipping point where cloud either stabilises or glaciates (see Sect. 3.2).

To achieve the target IWP, we set INP number concentration and freezing rate of INP appropriately. First, the INP number concentration is was by incorporating 2b bins that contained fractions x of dust and $(1-x)$ of ammonium bisulphate, where $x = 0.015$. The number concentration of dust containing particles is 238.5e3 and 9.75e3 kg^{-1} in accumulation and coarse modes, respectively. Here, the insoluble dust core (50 $\%$ of the dry mass) acts as the INP. The total number concentration of the aerosol, and thus also the droplet number concentration in cloud, is the same as in fixed ice number simulations (Sect. 3.1 and 3.2). Second, the freezing rate was adjust by setting the cosine of the contact angle of dust to $m_{is} = 0.57$ (Eq. A3 in Appendix A). Contact angle represent the angle between the ice embryo and the ice nucleus (IN) in an aqueous medium. These two parameters (x and m_{is}) were modified to reach the target IWP value in the prognostic ice simulation.

The simulation time for the prognostic ice run was set to 32 hours. The water paths of the mixed-phase cloud are quite stable after that. The simulation time of ICE4, used to compare with the prognostic run, was not extended any further from 24 hours since the cloud dissipates around 12 hours of simulation.

As in the ICE4 simulation, in the prognostic ice simulation, droplet freezing was set to start after a spinup of 2 hours. Figures 4a and 4b illustrate that the prognostic ice and ICE4 simulations have similar IWP and LWP during the first 8 hours. Hence, the targeting is successful and the initial conditions of the simulations match each other. After that, the prognostic ice simulation diverges from the ICE4 simulation.

Figure 4a shows that in the prognostic ice simulation LWP starts to increase after 4.5 hours of simulation. This is caused by a decrease of ice number concentration (Fig. 4c) to such a low level at which leaves more water vapour for condensation to liquid droplets. The same figure also depicts how the ice number concentration is set to a target value (simulation ICE4) and how the concentration is stable until the cloud dissipates. Figure 4d illustrates how the whole cloud with prognostic droplet freezing descends and how the ICE4 is affected by entrainment both below and above the cloud, cloud gets thinner and dissipates.

In the beginning of the prognostic ice run, domain mean of dust containing aerosols is approximately 27 L^{-1}. After 32 hours of simulation the same mean value is about 13 L^{-1}. Here, the loss of INPs limits the ice number concentration. The mixed-phase cloud persists because the ice number concentration can change. This is so-called self-adjustment of INPs which better reproduces observed evolution of mixed-phase clouds since usually they are more resilient in observations than in models (Andronache, 2017; Morrison et al., 2011a). The decrease of dust (INP) mass concentration in different hydrometeor types is shown in Fig. 5. Dust is an efficient ice nuclei so it will soon end up in ice crystals which are removed from the system by sedimentation (Fig. 5c). Free troposphere is the only source for the boundary layer dust, and the relevant mechanisms are

https://doi.org/10.5194/acp-2019-1182
Preprint. Discussion started: 28 January 2020

Atmospheric Chemistry and Physics Discussions

entrainment and large scale subsidence. Subsidence is described with a downward vertical velocity moving mass and energy. Entrainment in this case describes any other kind of mass exchange between cloud top and free troposphere. For instance, subsidence is 0.004 $\mathrm{m\ s^{-1}}$ at the cloud top and aerosol number concentration in dust containing b bins above the cloud is about 24000 $\mathrm{m^{-3}}$, so the dust aerosol flux from the free troposphere is approximately 100 $\mathrm{m^{-2}\ s^{-1}}$. Because radiative cooling is strengthening the supersaturation at the cloud top, the most CCN active part of these entrained dust containing particles can be activated immediately as cloud droplets. This can be seen as a higher dust mass concentration within cloud droplets in the upper layer of the cloud (Fig. 5b). If the temperature is low enough, these dust containing droplets will subsequently freeze during the following time steps and therefore takes part in preserving the mixed-phase cloud.

A more detailed examination of droplet activation and ice formation can be done by studying the time evolution of the size distribution. Figure 6 shows how different sized particles are partitioned between different hydrometeor types within the cloud layer. Figures 6c and 6d show how the larger particles freeze first and their number concentration decreases quickly as these particles deposit at the surface within falling ice hydrometeors and are removed from the system. Even though the entrainment from above is providing more particles, this is not fast enough to maintain the original concentration. Removal of the smaller IN is slower as those are less likely to activate as cloud droplets and the resulting droplets are also less likely to freeze due to the smaller dust core area. However, with time and because of continuous mixing of boundary layer eventually also the smaller IN particles are able to form cloud droplet within the strongest updrafts and formed droplets will freeze within the cloud. This will lead to stabilisation of aerosol size distribution. The increase in the total number of particles in bin 1 is a numerical artefact caused by the bin adjustment routine, which can move particles from one bin to another in order to keep the dry size within the predefined bin limits. When a large fraction of particles in bin 2 are activated as cloud droplets, some of the remaining are moved to the smaller bin to avoid numerical problems.

Figures 7a and 7b illustrate, how super-cooled liquid droplets are dominant in the upper layers of the mixed-phase cloud compared to ice crystals. Here the total ice number concentration stabilises at approximately 0.44 $\mathrm{L^{-1}}$, whereas it is obvious from Sect. 3.2 that a much higher concentration is needed to completely glaciate the cloud. Similarly, the cloud droplet number concentration is approximately 175 $\mathrm{cm{-}3}$. Although our original goal was not to compare directly against observation, these values are in good line with aircraft observations (Flight F31) of this ISDAC case. The observed ice and cloud droplet number concentration are 0.35 $\mathrm{L^{-1}}$ and 185 $\mathrm{cm{-}3}$, respectively (McFarquhar et al., 2011; Savre and Ekman, 2015). Concentration is also approximately two orders of magnitude less than the number concentration of efficient IN above the cloud layer. From that we can estimate that the concentration of IN entraining from above the cloud should be in the order of 0.1 to 1.0 $\mathrm{cm{-}3}$ to glaciate the cloud.

Figure 7c further illustrates an interesting behaviour of ice particle formation. In the beginning of the simulation ice particles are formed throughout the cloud, but later the most intensive formation takes place at the top of cloud where fresh IN particles are entrained into the cloud layer. However, the maximum supersaturation in these entraining downdrafts is so low, that only the largest particles are able to form cloud droplets and consequently freeze. The smaller ones penetrate through the cloud layer as interstitial aerosol particles, and are able to form cloud droplets and ice particles at the cloud base when they are recirculated back to the cloud. This can be well seen at the end of simulation as there is two peaks in vertical profile of freezing rate.

https://doi.org/10.5194/acp-2019-1182
Preprint. Discussion started: 28 January 2020


Atmospheric Chemistry and Physics Discussions

Such phenomena can be only simulated with explicit calculation of in-cloud supersaturation and representation of aerosol size distribution and chemical composition like is done in UCLALES-SALSA. Compared to Savre and Ekman (2015), where most intensive freezing is at the cloud top, in UCLALES-SALSA droplet freezing occurs throughout the cloud Overall, Figs. 6 and 7c nicely demonstrate how the relative fractions of particles in different hydrometeors are size dependent and how sectional description for aerosols is required to be able to simulate such processes in LES models.

4 Conclusions

In this study we have extended our large-eddy model UCLALES-SALSA (Tonttila et al., 2017) for ice and mixed-phase clouds. The model has an exceptionally detailed sectional aerosol description for both aerosol number and chemical composition, which makes this model suitable for examining aerosol-cloud interactions and dynamics. Specifically, this allows the description of an ice nucleation active material such as mineral dust, which can be used in calculating ice formation rates from the nucleation theory.

As the first step, we compared our model predictions with those from a mixed-phase cloud model intercomparison study (Ovchinnikov et al., 2014) to confirm the accuracy of the newly implemented ice microphysics. In this simplified model intercomparison setup, where any cloud droplet will freeze until a specified ice number concentration (from zero up to four particles per liter) is reached, the focus is on cloud dynamics. In agreement with Ovchinnikov et al. (2014) and several other studies (e.g., Klein et al., 2009; Morrison et al., 2011b; Stevens et al., 2018) we conclude that microphysical details such as the fact that dry particle size is tracked in UCLALES-SALSA while most other sectional models track the ice particle size have an impact on predictions. Such details become more important close to the tipping point where the further addition of ice particles leads to the rapid glaciation of the cloud.

In the second part, we constructed a case where ice formation is modelled using a heterogeneous ice nucleation scheme and a prognostic ice nucleating particle population containing mineral dust. This so-called prognostic ice simulation was designed so that it matched with the previous fixed ice number concentration simulation where the cloud was close to the tipping point. When the simulation with fixed ice concentration showed a complete glaciation after about 12 hours, the prognostic ice simulation reached an equilibrium state which lasted up to end of the 32 hour simulation. With this the prognostic simulation showed the importance of the self-adjustment of ice nucleation active particles. This is in good agreement with a observational study where resilient mixed-phase clouds are seen together with relatively high ice nuclei concentrations (Filioglou et al., 2019).

Further examination of the prognostic ice simulation revealed that the efficient IN entrained from the free troposphere are able to maintain the mixed phase cloud with ice particle number concentration on average 0.1-0.2 % of the IN concentration above the cloud. These entrained particles do not immediately form ice particles in the cloud top. The detailed analysis of the model outputs reveals how particle size and supersaturation-dependent cloud activation eventually control the formation of ice through immersion freezing. Part of entrained IN particles penetrate through the cloud as interstitial particles, get mixed

https://doi.org/10.5194/acp-2019-1182
Preprint. Discussion started: 28 January 2020

Atmospheric Chemistry and Physics Discussions

within boundary layer air and contribute ice formation later when recycled back to the cloud. Thus the entrainment process is maintaining IN concentration in the whole boundary layer.

This study emphasizes the benefits of the detailed aerosol-cloud-ice module within a LES model. In fact, UCLALES-SALSA is one of the few cloud scale models (Fridlind et al., 2012; Khain et al., 2004; Savre and Ekman, 2015; Fu and Xue, 2017) where details about aerosol and cloud droplet chemical composition can be utilized by using the particle level theoretical understanding about ice nucleation. The model will be a useful tool for the mixed-phase cloud research, which has started to attract more widespread interest.

Code and data availability. The source code of the model is available from Github:
https://github.com/UCLALES-SALSA/UCLALES-SALSA, Release tag: IceV1.0, Release name: Ice microphysics V1.0.
Model output data and figure scripts: http://urn.fi/urn:nbn:fi:att:5144df1e-4cdf-4d5a-af46-a545ebaa4460

Appendix A: Immersion freezing

The rate J of heterogeneous germ formation by immersion freezing is a function of T temperature in kelvins, r_N radius of insoluble substrate and S_w equilibrium saturation ratio at droplet surface based on Kohler theory and is determined as

$$J(T, r_N, S_w) = C_{het}\left[-\frac{\Delta F_{act} - \Delta F_{cr}}{kT}\right](\mathrm{s}^{-1}),$$
$$C_{het} = \frac{kT}{h} c_{1s} 4\pi r_N^2, \tag{A1}$$

where k and h Boltzmann's and Planck's constants, ΔF_{act} is the activation energy at the solution-ice interface, ΔF_{cr} is the critical energy of germ formation, C_{het} is the normalizing function, r_N the radius of an insoluble fraction of an aerosol particle (IN), and c_{1s} is the concentration of water molecules adsorbed on $1\mathrm{cm}^{-2}$ of a surface (Eq. 2.1 Khvorostyanov and Curry (2004)). Used parameter values are $C = 1.7 \times 10.999850^{10}$ N m^{-2} and $c_{1s} = 1 \times 10^{19}$ m^{-2}.

Activation energy ΔF_{act} is calculated based on Eq. 15 in Jeffery and Austin (1997)

$$\Delta F_{act} = RT\left(\frac{B}{T - T_*} - \ln\frac{D_*}{D_0}\right)/N_A, \tag{A2}$$

where T is temperature in kelvin, R is the molar gas constant and N_A is the Avogadro constant and parameter values $B = 347$, $T_* = 177$, $D_* = 4.17$ and $D_0 = 349$ for $p = 1$ bar are gained from Table 2 in Khvorostyanov and Curry (2004).

Critical energy is based on Eq. 2.10 in Khvorostyanov and Curry (2000)

$$\Delta F_{cr} = \frac{4\pi}{3}\sigma_{is} r_{cr}^2 f(m_{is}, x) - \alpha r_N^2 (1 - m_{is}), \tag{A3}$$

where

$$\sigma_{is} = 28 \times 10^{-3} + 0.25 T_c \times 10^{-3}, \tag{A4}$$

https://doi.org/10.5194/acp-2019-1182
Preprint. Discussion started: 28 January 2020

Atmospheric Chemistry and Physics Discussions

where T_c is temperature in Celsius degrees (Khvorostyanov and K. Sassen, 1998);

$$r_{cr} = \frac{\sigma_{is}}{\rho_{ice} L_m^{ef} \ln(\frac{T_0}{T} S_W^G) - C\epsilon^2}, \tag{A5}$$

where $\rho_{ice} = 900$ (kg m^{-3} is the density of ice, $T_0 = 273.15$ K;

$$L_m^{ef} = (79.7 + 0.708 T_c - 2.5 \times 10^{-3} \times T_c^2) \times 4.186810^3 \tag{A6}$$

is the effective latent heat of melting (Eq. 6 Khvorostyanov and K. Sassen (1998)); dimensionless parameter

$$G = \frac{RT}{M_w L_m^{ef}}, \tag{A7}$$

where M_w is the molar mass of water (Eq. 2.7 in Khvorostyanov and Curry (2000)).

The shape factor f is defined as a function of ratio $x = r_N/r_{cr}$ and $m = m_{is}$. It is gained from Eq. 2.9 in Khvorostyanov and Curry (2000), originally from Fletcher (1962),

$$2f(m,x) = 1 + [(1-mx)/\phi]^3 + x^3(2 - 3\psi + \psi^3) + 3mx^3(\psi - 1), \psi = (x-m)/\phi, \phi = (1 - 2mx + x^2)^{1/2} \tag{A8}$$

Case dependent parameters ϵ, elastic strain produced in ice embryo by the insoluble substrate; α, relative area of active sites; m_{is}, cosine of the contact angle; are defined in our results 3.3 to be

$$\begin{aligned} \epsilon &= 0 \\ \alpha &= 0 \\ m_{is} &= 0.57. \end{aligned} \tag{A9}$$

The m_{is} was used as targeting parameter since the simulation tests were found to be very sensitive for this parameter. Other case dependent parameters ϵ and α were not altered and had their default values.

Author contributions. Ahola made the simulations with the help from Raatikainen. Ahola analysed the data with help from Raatikainen and Romakkaniemi. Ahola wrote the paper with comments from Kokkola, Korhonen, Raatikainen, Romakkaniemi and Tonttila. Ahola, Raatikainen, Tonttila, Kokkola and Romakkaniemi have contributed in developing the UCLALES-SALSA model. Korhonen supervised the project.

Competing interests. The authors declare that they have no conflict of interest.

https://doi.org/10.5194/acp-2019-1182
Preprint. Discussion started: 28 January 2020

Acknowledgements. This study has been funded by the European Research Council (Consolidator Grant 646857). Tomi Raatikainen acknowledges Academy of Finland for Research Fellow funding (grant number 322532). Dr. Mikhail Ovchinnikov is acknowledged for providing the simulation data of Ovchinnikov et al. (2014).

https://doi.org/10.5194/acp-2019-1182
Preprint. Discussion started: 28 January 2020

Atmospheric Chemistry and Physics Discussions

References

Interactions among aerosols, clouds, and climate of the Arctic Ocean.

Andronache, C.: Mixed-phase Clouds: Observations and Modeling, Elsevier, Saint Louis, Retrieved\from\https://ebookcentral.proquest.com/lib/fmi/detail.action?docID=5064425, proQuest Ebook Central, 2017.

Atkinson, J. D., Murray, B. J., Woodhouse, M. T., Whale, T. F., Baustian, K. J., Carslaw, K. S., Dobbie, S., O'Sullivan, D., and Malkin, T. L.: The importance of feldspar for ice nucleation by mineral dust in mixed-phase clouds, Nature, 498, 355, https://doi.org/10.1038/nature12278, 2013.

Avramov, A. and Harrington, J. Y.: Influence of parameterized ice habit on simulated mixed phase Arctic clouds, J. Geophys. Res, 115, https://doi.org/10.1029/2009JD012108, 2010.

Cox, S. K.: Cirrus Clouds and the Climate, J. Atmospheric Sci., 28, 1513–1515, https://doi.org/10.1175/1520-0469(1971)028<1513:CCATC>2.0.CO;2, 1971.

Curry, J. A., Pinto, J. O., Benner, T., and Tschudi, M.: Evolution of the cloudy boundary layer during the autumnal freezing of the Beaufort Sea, J. Geophys. Res, 102, 13 851–13 860, https://doi.org/10.1029/96JD03089, 1997.

de Boer, G., Eloranta, E. W., and Shupe, M. D.: Arctic Mixed-Phase Stratiform Cloud Properties from Multiple Years of Surface-Based Measurements at Two High-Latitude Locations, J. Atmospheric Sci., 66, 2874–2887, https://doi.org/10.1175/2009JAS3029.1, 2009.

DeMott, P. J., Möhler, O., Stetzer, O., Vali, G., Levin, Z., Petters, M. D., Murakami, M., Leisner, T., Bundke, U., Klein, H., Kanji, Z. A., Cotton, R., Jones, H., Benz, S., Brinkmann, M., Rzesanke, D., Saathoff, H., Nicolet, M., Saito, A., Nillius, B., Bingemer, H., Abbatt, J., Ardon, K., Ganor, E., Georgakopoulos, D. G., and Saunders, C.: Resurgence in Ice Nuclei Measurement Research, Bull. Am. Meteorol. Soc., 92, 1623–1635, https://doi.org/10.1175/2011BAMS3119.1, 2011.

Filioglou, M., Mielonen, T., Balis, D., Giannakaki, E., Arola, A., Kokkola, H., Komppula, M., and Romakkaniemi, S.: Aerosol Effect on the Cloud Phase of Low-Level Clouds Over the Arctic, J. Geophys. Res. Atmos., 124, 7886–7899, https://doi.org/10.1029/2018JD030088, 2019.

Fletcher, N. H.: The physics of rainclouds. By N. H. Fletcher. Cambridge University Press, Pp. x, 386; 99 Figures; 6 Plates. 65s, Q. J. Royal Meteorol. Soc., 88, 559–559, https://doi.org/10.1002/qj.49708837821, 1962.

Fridlind, A. M., van Diedenhoven, B., Ackerman, A. S., Avramov, A., Mrowiec, A., Morrison, H., Zuidema, P., and Shupe, M. D.: A FIRE-ACE/SHEBA Case Study of Mixed-Phase Arctic Boundary Layer Clouds: Entrainment Rate Limitations on Rapid Primary Ice Nucleation Processes, J. Atmospheric Sci., 69, 365–389, https://doi.org/10.1175/JAS-D-11-052.1, 2012.

Fu, Q. and Liou, K. N.: Parameterization of the Radiative Properties of Cirrus Clouds, J. Atmospheric Sci., 50, 2008–2025, https://doi.org/10.1175/1520-0469(1993)050<2008:POTRPO>2.0.CO;2, 1993.

Fu, S. and Xue, H.: The Effect of Ice Nuclei Efficiency on Arctic Mixed-Phase Clouds from Large-Eddy Simulations, J. Atmospheric Sci., 74, 3901–3913, https://doi.org/10.1175/JAS-D-17-0112.1, 2017.

Harrington, J. Y., Reisin, T., Cotton, W. R., and Kreidenweis, S. M.: Cloud resolving simulations of Arctic stratus: Part II: Transition-season clouds, Atmospheric Res., 51, 45 – 75, https://doi.org/https://doi.org/10.1016/S0169-8095(98)00098-2, 1999.

Hobbs, P. V. and Rangno, A. L.: Microstructures of low and middle-level clouds over the Beaufort Sea, Q. J. Royal Meteorol. Soc., 124, 2035–2071, https://doi.org/10.1002/qj.49712455012, 1998.

https://doi.org/10.5194/acp-2019-1182
Preprint. Discussion started: 28 January 2020

Hoose, C., Kristjánsson, J. E., Chen, J.-P., and Hazra, A.: A Classical-Theory-Based Parameterization of Heterogeneous Ice Nucleation by Mineral Dust, Soot, and Biological Particles in a Global Climate Model, J. Atmospheric Sci., 67, 2483–2503, https://doi.org/10.1175/2010JAS3425.1, 2010.

Jacobson, M. Z.: Fundamentals of Atmospheric Modeling, Cambridge University Press, 2nd edn., https://doi.org/10.1017/CBO9781139165389, 2005.

Jeffery, C. A. and Austin, P. H.: Homogeneous nucleation of supercooled water: Results from a new equation of state, J. Geophys. Res. Atmos., 102, 25 269–25 279, https://doi.org/10.1029/97JD02243, 1997.

Jiang, H., Cotton, W. R., Pinto, J. O., Curry, J. A., and Weissbluth, M. J.: Cloud Resolving Simulations of Mixed-Phase Arctic Stratus Observed during BASE: Sensitivity to Concentration of Ice Crystals and Large-Scale Heat and Moisture Advection, J. Atmospheric Sci., 57, 2105–2117, https://doi.org/10.1175/1520-0469(2000)057<2105:CRSOMP>2.0.CO;2, 2000.

Khain, A., Pokrovsky, A., Pinsky, M., Seifert, A., and Phillips, V.: Simulation of Effects of Atmospheric Aerosols on Deep Turbulent Convective Clouds Using a Spectral Microphysics Mixed-Phase Cumulus Cloud Model. Part I: Model Description and Possible Applications, J. Atmospheric Sci., 61, 2963–2982, https://doi.org/10.1175/JAS-3350.1, 2004.

Khvorostyanov, V. and K. Sassen, a.: Khvorostyanov V., and K. Sassen, 1998. Towards the theory of homogeneous nucleation and its parameterization for cloud models. Geophys. Res. Lett., 25, No 16, 3155-3158., Geophys. Res. Lett., 25, 3155–3158, https://doi.org/10.1029/98GL02332, 1998.

Khvorostyanov, V. I. and Curry, J. A.: Khvorostyanov, V. I., and J. A. Curry, 2000. A new theory of heterogeneous ice nucleation for application in cloud and climate models. Geophys. Res. Lett., 27, 4081-4084., Geophys. Res. Lett., 27, 4081–4084, https://doi.org/10.1029/1999GL011211, 2000.

Khvorostyanov, V. I. and Curry, J. A.: The Theory of Ice Nucleation by Heterogeneous Freezing of Deliquescent Mixed CCN. Part I: Critical Radius, Energy, and Nucleation Rate, J. Atmospheric Sci., 61, 2676–2691, https://doi.org/10.1175/JAS3266.1, 2004.

Kiselev, A., Bachmann, F., Pedevilla, P., Cox, S. J., Michaelides, A., Gerthsen, D., and Leisner, T.: Active sites in heterogeneous ice nucleation—the example of K-rich feldspars, Science, 355, 367–371, https://doi.org/10.1126/science.aai8034, 2017.

Klein, S. A., McCoy, R. B., Morrison, H., Ackerman, A. S., Avramov, A., de Boer, G., Chen, M., Cole, J. N. S., Del Genio, A. D., Falk, M., Foster, M. J., Fridlind, A., Golaz, J.-C., Hashino, T., Harrington, J. Y., Hoose, C., Khairoutdinov, M. F., Larson, V. E., Liu, X., Luo, Y., McFarquhar, G. M., Menon, S., Neggers, R. A. J., Park, S., Poellot, M. R., Schmidt, J. M., Sednev, I., Shipway, B. J., Shupe, M. D., Spangenberg, D. A., Sud, Y. C., Turner, D. D., Veron, D. E., von Salzen, K., Walker, G. K., Wang, Z., Wolf, A. B., Xie, S., Xu, X.-M., Yang, F., and Zhang, G.: Intercomparison of model simulations of mixed-phase clouds observed during the ARM Mixed-Phase Arctic Cloud Experiment. Part I: Single-layer cloud, Q. J. Roy. Meteorol. Soc., 135, 979–1002, https://doi.org/10.1002/qj.416, 2009.

Knight, N. C. and Heymsfield, A. J.: Measurement and Interpretation of Hailstone Density and Terminal Velocity, J. Atmospheric Sci., 40, 1510–1516, https://doi.org/10.1175/1520-0469(1983)040<1510:MAIOHD>2.0.CO;2, 1983.

Kokkola, H., Korhonen, H., Lehtinen, K. E. J., Makkonen, R., Asmi, A., Järvenoja, S., Anttila, T., Partanen, A.-I., Kulmala, M., Järvinen, H., Laaksonen, A., and Kerminen, V.-M.: SALSA – a Sectional Aerosol module for Large Scale Applications, Atmospheric Chem. Phys., 8, 2469–2483, https://doi.org/10.5194/acp-8-2469-2008, 2008.

Kokkola, H., Kühn, T., Laakso, A., Bergman, T., Lehtinen, K. E. J., Mielonen, T., Arola, A., Stadtler, S., Korhonen, H., Ferrachat, S., Lohmann, U., Neubauer, D., Tegen, I., Siegenthaler-Le Drian, C., Schultz, M. G., Bey, I., Stier, P., Daskalakis, N., Heald, C. L., and Romakkaniemi, S.: SALSA2.0: The sectional aerosol module of the aerosol–chemistry–climate model ECHAM6.3.0-HAM2.3-MOZ1.0, Geosci. Model Dev., 11, 3833–3863, https://doi.org/10.5194/gmd-11-3833-2018, 2018.

https://doi.org/10.5194/acp-2019-1182
Preprint. Discussion started: 28 January 2020

Lebo, Z. J., Johnson, N. C., and Harrington, J. Y.: Radiative influences on ice crystal and droplet growth within mixed-phase stratus clouds, J. Geophys. Res. Atmos., 113, https://doi.org/10.1029/2007JD009262, https://agupubs.onlinelibrary.wiley.com/doi/abs/10.1029/2007JD009262, 2008.

Li, Z., Xue, H., and Yang, F.: A modeling study of ice formation affected by aerosols, J. Geophys. Res. Atmos., 118, 11,213–11,227, https://doi.org/10.1002/jgrd.50861, 2013.

McFarquhar, G. M., Ghan, S., Verlinde, J., Korolev, A., Strapp, J. W., Schmid, B., Tomlinson, J. M., Wolde, M., Brooks, S. D., Cziczo, D., Dubey, M. K., Fan, J., Flynn, C., Gultepe, I., Hubbe, J., Gilles, M. K., Laskin, A., Lawson, P., Leaitch, W. R., Liu, P., Liu, X., Lubin, D., Mazzoleni, C., Macdonald, A.-M., Moffet, R. C., Morrison, H., Ovchinnikov, M., Shupe, M. D., Turner, D. D., Xie, S., Zelenyuk, A., Bae, K., Freer, M., and Glen, A.: Indirect and Semi-direct Aerosol Campaign, Bull. Am. Meteorol. Soc., 92, 183–201, https://doi.org/10.1175/2010BAMS2935.1, 2011.

Morrison, H.: On the robustness of aerosol effects on an idealized supercell storm simulated with a cloud system-resolving model, Atmospheric Chem. Phys., 12, 7689–7705, https://doi.org/10.5194/acp-12-7689-2012, https://www.atmos-chem-phys.net/12/7689/2012/, 2012.

Morrison, H., Shupe, M. D., Pinto, J. O., and Curry, J. A.: Possible roles of ice nucleation mode and ice nuclei depletion in the extended lifetime of Arctic mixed-phase clouds, Geophys. Res. Lett., 32, https://doi.org/10.1029/2005GL023614, 2005.

Morrison, H., de Boer, G., Feingold, G., Harrington, J., Shupe, M. D., and Sulia, K.: Resilience of persistent Arctic mixed-phase clouds, Nat. Geosci., 5, 11 EP, https://doi.org/10.1038/ngeo1332, review Article, 2011a.

Morrison, H., Zuidema, P., Ackerman, A. S., Avramov, A., de Boer, G., Fan, J., Fridlind, A. M., Hashino, T., Harrington, J. Y., Luo, Y., Ovchinnikov, M., and Shipway, B.: Intercomparison of cloud model simulations of Arctic mixed-phase boundary layer clouds observed during SHEBA/FIRE-ACE, J. Adv. Model. Earth Sys., 3, M06 003, https://doi.org/10.1029/2011MS000066, 2011b.

Norgren, M. S., de Boer, G., and Shupe, M. D.: Observed aerosol suppression of cloud ice in low-level Arctic mixed-phase clouds, Atmospheric Chem. Phys., 18, 13 345–13 361, https://doi.org/10.5194/acp-18-13345-2018, https://www.atmos-chem-phys.net/18/13345/2018/, 2018.

Ovchinnikov, M., Ackerman, A. S., Avramov, A., Cheng, A., Fan, J., Fridlind, A. M., Ghan, S., Harrington, J., Hoose, C., Korolev, A., McFarquhar, G. M., Morrison, H., Paukert, M., Savre, J., Shipway, B. J., Shupe, M. D., Solomon, A., and Sulia, K.: Intercomparison of large-eddy simulations of Arctic mixed-phase clouds: Importance of ice size distribution assumptions, J. Adv. Model. Earth Sys., 6, 223–248, https://doi.org/10.1002/2013MS000282, 2014.

Petters, M. D. and Kreidenweis, S. M.: A single parameter representation of hygroscopic growth and cloud condensation nucleus activity, Atmospheric Chem. Phys., 7, 1961–1971, https://doi.org/10.5194/acp-7-1961-2007, 2007.

Petters, M. D., Prenni, A. J., Kreidenweis, S. M., DeMott, P. J., Matsunaga, A., Lim, Y. B., and Ziemann, P. J.: Chemical aging and the hydrophobic-to-hydrophilic conversion of carbonaceous aerosol, Geophys. Res. Lett., 33, https://doi.org/10.1029/2006GL027249, 2006.

Phillips, V. T. J., DeMott, P. J., and Andronache, C.: An Empirical Parameterization of Heterogeneous Ice Nucleation for Multiple Chemical Species of Aerosol, J. Atmospheric Sci., 65, 2757–2783, https://doi.org/10.1175/2007JAS2546.1, 2008.

Pinto, J. O.: Autumnal Mixed-Phase Cloudy Boundary Layers in the Arctic, J. Atmospheric Sci., 55, 2016–2038, https://doi.org/10.1175/1520-0469(1998)055<2016:AMPCBL>2.0.CO;2, 1998.

Rangno, A. L. and Hobbs, P. V.: Ice particles in stratiform clouds in the Arctic and possible mechanisms for the production of high ice concentrations, J. Geophys. Res. Atmos., 106, 15 065–15 075, https://doi.org/10.1029/2000JD900286, https://agupubs.onlinelibrary.wiley.com/doi/abs/10.1029/2000JD900286, 2001.

https://doi.org/10.5194/acp-2019-1182
Preprint. Discussion started: 28 January 2020

Atmospheric Chemistry and Physics Discussions

Rauber, R. M. and Tokay, A.: An Explanation for the Existence of Supercooled Water at the Top of Cold Clouds, J. Atmospheric Sci., 48, 1005–1023, https://doi.org/10.1175/1520-0469(1991)048<1005:AEFTEO>2.0.CO;2, 1991.

Savre, J. and Ekman, A. M. L.: Large-eddy simulation of three mixed-phase cloud events during ISDAC: Conditions for persistent heterogeneous ice formation, J. Geophys. Res. Atmos., 120, 7699–7725, https://doi.org/10.1002/2014JD023006, 2015.

Shupe, M. D., Matrosov, S. Y., and Uttal, T.: Arctic Mixed-Phase Cloud Properties Derived from Surface-Based Sensors at SHEBA, J. Atmospheric Sci., 63, 697–711, https://doi.org/10.1175/JAS3659.1, 2006.

Solomon, S., Qin, D., Manning, M., Marquis, M., Averyt, K., Tignor, M. M. B., L., M. J. H., and Chen, Z.: Climate Change 2007: The Physical Science Basis, Cambridge University Press, U. K., and New York, NY, USA, 2007.

Stevens, B. and Feingold, G.: Untangling aerosol effects on clouds and precipitation in a buffered system, Nature, 461, 607–613, https://doi.org/10.1038/nature08281, https://doi.org/10.1038/nature08281, 2009.

Stevens, B., Moeng, C.-H., and Sullivan, P. P.: Large-Eddy Simulations of Radiatively Driven Convection: Sensitivities to the Representation of Small Scales, J. Atmospheric Sci., 56, 3963–3984, https://doi.org/10.1175/1520-0469(1999)056<3963:LESORD>2.0.CO;2, 1999.

Stevens, B., Moeng, C.-H., Ackerman, A. S., Bretherton, C. S., Chlond, A., de Roode, S., Edwards, J., Golaz, J.-C., Jiang, H., Khairoutdinov, M., Kirkpatrick, M. P., Lewellen, D. C., Lock, A., Müller, F., Stevens, D. E., Whelan, E., and Zhu, P.: Evaluation of Large-Eddy Simulations via Observations of Nocturnal Marine Stratocumulus, Mon. Weather Rev., 133, 1443–1462, https://doi.org/10.1175/MWR2930.1, 2005.

Stevens, R. G., Loewe, K., Dearden, C., Dimitrelos, A., Possner, A., Eirund, G. K., Raatikainen, T., Hill, A. A., Shipway, B. J., Wilkinson, J., Romakkaniemi, S., Tonttila, J., Laaksonen, A., Korhonen, H., Connolly, P., Lohmann, U., Hoose, C., Ekman, A. M. L., Carslaw, K. S., and Field, P. R.: A model intercomparison of CCN-limited tenuous clouds in the high Arctic, Atmospheric Chem. Phys., 18, 11 041–11 071, https://doi.org/10.5194/acp-18-11041-2018, 2018.

Stokes, R. H. and Robinson, R. A.: Interactions in Aqueous Nonelectrolyte Solutions. I. Solute-Solvent Equilibria, J. Chem. Phys., 70, 2126–2131, https://doi.org/10.1021/j100879a010, 1966.

Tonttila, J., Maalick, Z., Raatikainen, T., Kokkola, H., Kühn, T., and Romakkaniemi, S.: UCLALES–SALSA v1.0: a large-eddy model with interactive sectional microphysics for aerosol, clouds and precipitation, Geosci. Model Dev., 10, 169–188, https://doi.org/10.5194/gmd-10-169-2017, 2017.

Verlinde, J., Harrington, J. Y., McFarquhar, G. M., Yannuzzi, V. T., Avramov, A., Greenberg, S., Johnson, N., Zhang, G., Poellot, M. R., Mather, J. H., Turner, D. D., Eloranta, E. W., Zak, B. D., Prenni, A. J., Daniel, J. S., Kok, G. L., Tobin, D. C., Holz, R., Sassen, K., Spangenberg, D., Minnis, P., Tooman, T. P., Ivey, M. D., Richardson, S. J., Bahrmann, C. P., Shupe, M., DeMott, P. J., Heymsfield, A. J., and Schofield, R.: The Mixed-Phase Arctic Cloud Experiment, Bull. Am. Meteorol. Soc., 88, 205–222, https://doi.org/10.1175/BAMS-88-2-205, 2007.

Zuidema, P., Baker, B., Han, Y., Intrieri, J., Key, J., Lawson, P., Matrosov, S., Shupe, M., Stone, R., and Uttal, T.: An Arctic Springtime Mixed-Phase Cloudy Boundary Layer Observed during SHEBA, J. Atmospheric Sci., 62, 160–176, https://doi.org/10.1175/JAS-3368.1, 2005.

https://doi.org/10.5194/acp-2019-1182
Preprint. Discussion started: 28 January 2020

Atmospheric Chemistry and Physics Discussions

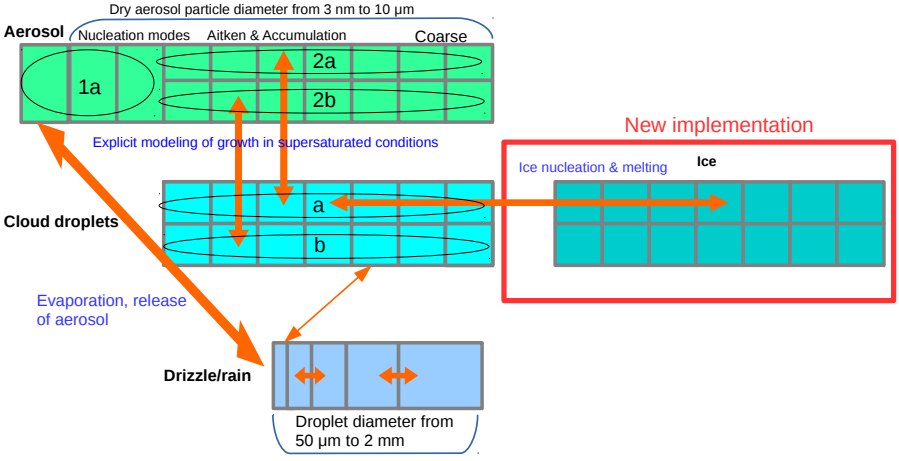

Figure 1. Bin scheme of UCLALES-SALSA with newly implemented particles, see also Fig. 1 in Tonttila et al. (2017).

https://doi.org/10.5194/acp-2019-1182
Preprint. Discussion started: 28 January 2020

Atmospheric Chemistry and Physics Discussions

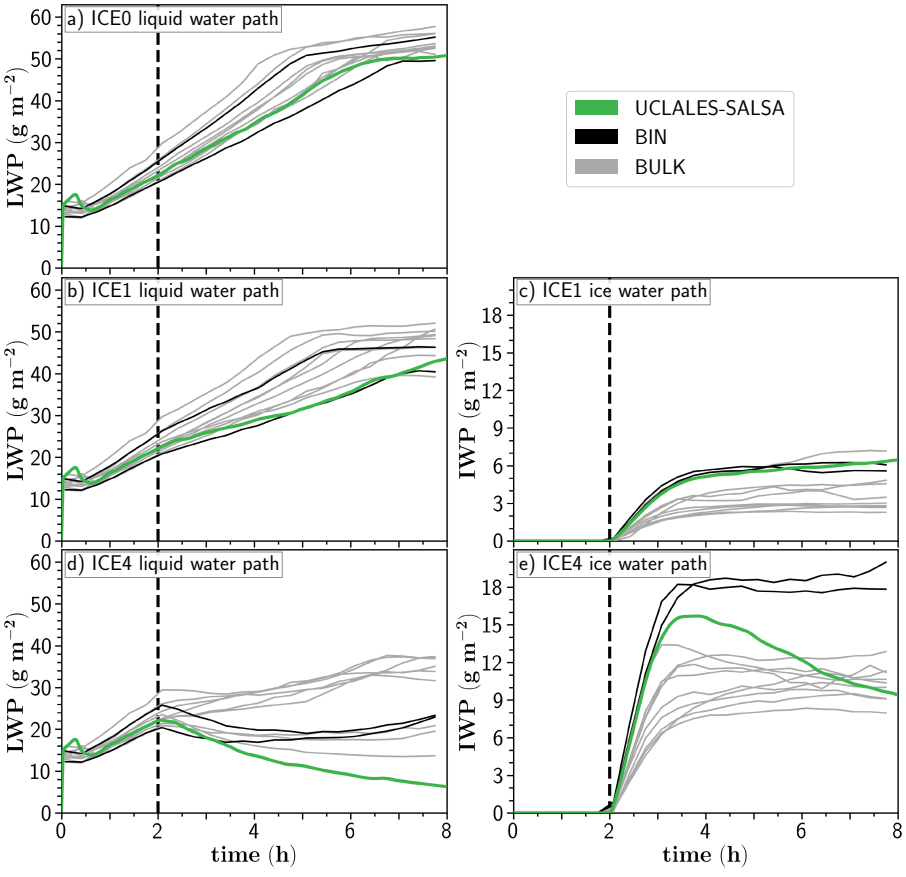

Figure 2. Liquid and ice water path time series in UCLALES-SALSA simulations with fixed ice number concentration of 0, 1 and 4 L^{-1} (ICE0, ICE1, ICE4 respectively). Black and grey lines show results in the Ovchinnikov et al. (2014) study.

https://doi.org/10.5194/acp-2019-1182
Preprint. Discussion started: 28 January 2020

Atmospheric Chemistry and Physics Discussions

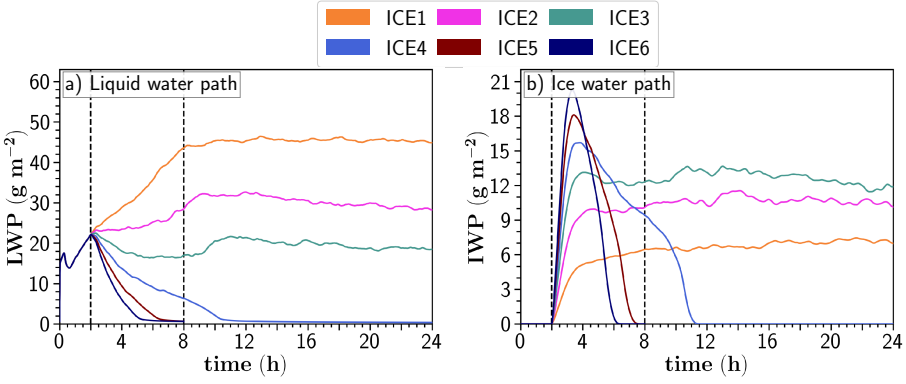

Figure 3. Liquid and ice water path time series in UCLALES-SALSA simulations with fixed ice number concentrations of 1, 2, 3, 4, 5 and 6 L^{-1} (ICE1, ICE2, ICE3, ICE4, ICE5 and ICE6, respectively).

https://doi.org/10.5194/acp-2019-1182
Preprint. Discussion started: 28 January 2020

Atmospheric Chemistry and Physics Discussions

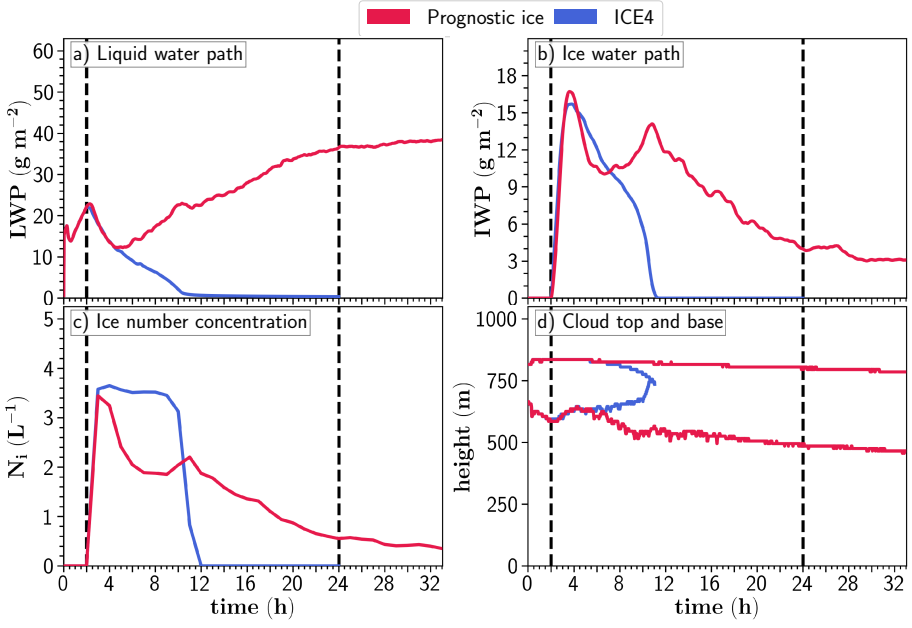

Figure 4. Time series of water paths and mean ice number concentration in icy regions of UCLALES-SALSA simulation of 48 hours with prognostic droplet freezing (Prognostic ice) compared with UCLALES-SALSA simulation of 24 hours with fixed ice number concentration of 4 L^{-1} (ICE4).

https://doi.org/10.5194/acp-2019-1182
Preprint. Discussion started: 28 January 2020

Atmospheric Chemistry and Physics Discussions

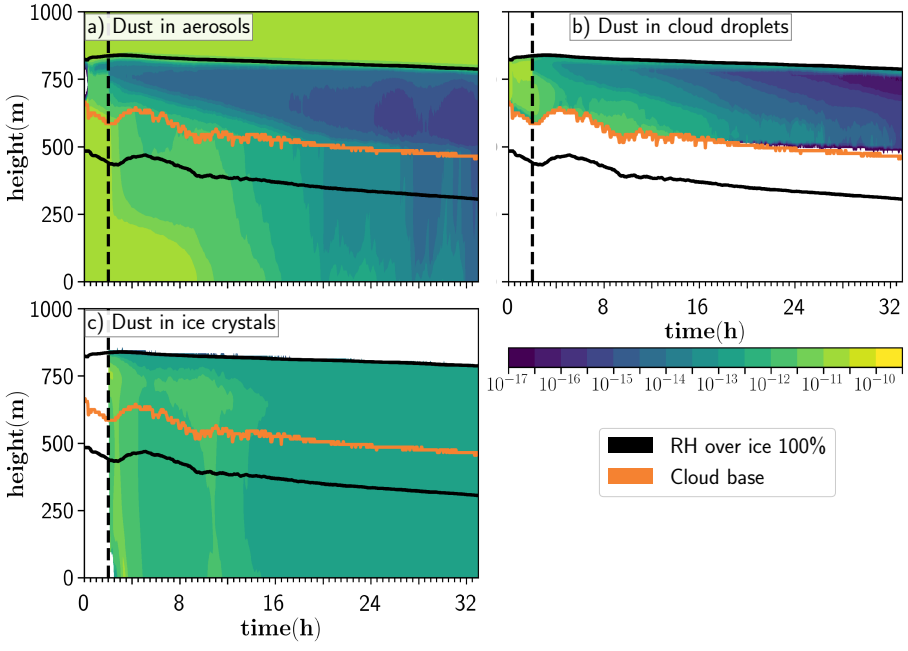

Figure 5. Logaritmic total mass mixing ratios (kg kg^{-1}) of dust in different hydrometeors given as cloud profile time series in UCLALES-SALSA simulation from the prognostic ice simulation. Cloud top is not plotted to keep the figure clearer because it is practically the same as upper RHi line.

https://doi.org/10.5194/acp-2019-1182
Preprint. Discussion started: 28 January 2020

Atmospheric Chemistry and Physics Discussions

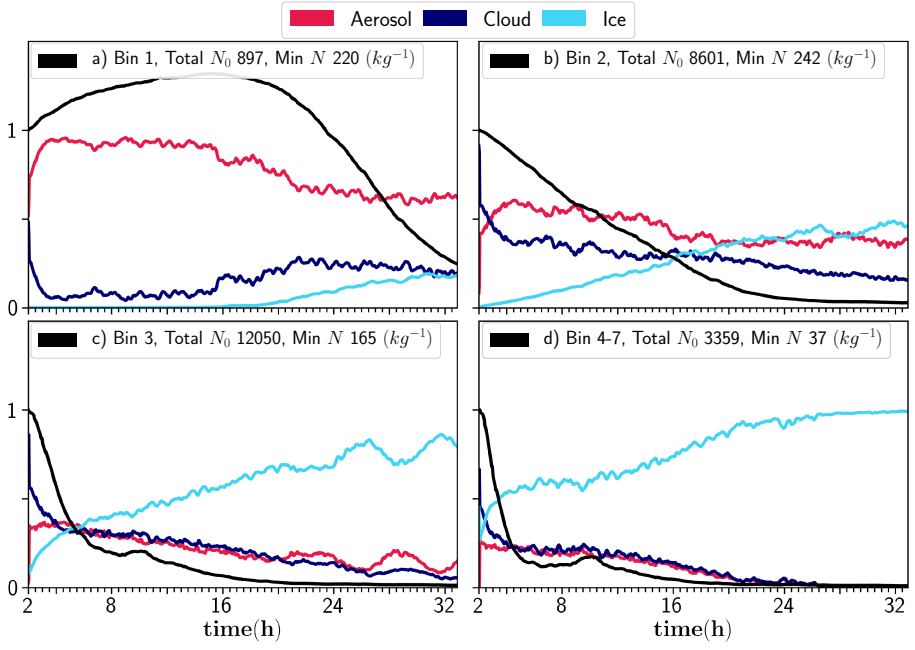

Figure 6. Relative portions of hydrometeors at each time step in the cloud layer. Cloud layer is defined when both cloud liquid water and ice mixing ratios are over 0.001 (g kg^{-1}). Black line represents relative change of the total number concentration in each bin.

https://doi.org/10.5194/acp-2019-1182
Preprint. Discussion started: 28 January 2020

Atmospheric Chemistry and Physics Discussions

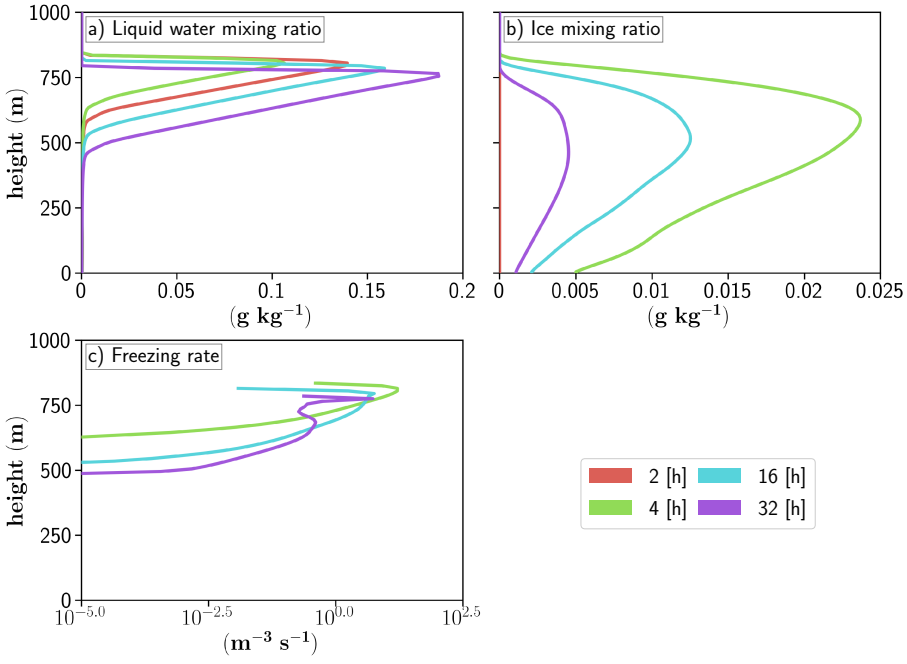

Figure 7. Vertical profiles of liquid water and ice and freezing rate of droplets (nucleation rate) UCLALES-SALSA simulation with prognostic droplet freezing.